

Experiments on Jerk-Limited Slew Maneuvers of a Flexible Spacecraft

Jae-Jun Kim* and Brij N. Agrawal †

Department of Mechanical and Astronautical Engineering

Naval Postgraduate School, Monterey, CA 93943

In this paper, experimental verifications of various jerk-limited control designs are presented. The focus is on a large slew maneuver of a flexible spacecraft where the fast and accurate pointing is required at the end of the maneuver. Various control profiles are investigated including input shaping and jerk-limited optimal control profiles, especially to account the effect of jerk in the control profile. The control design is verified by the experiment using the Flexible Spacecraft Simulator (FSS).

I. Introduction

Space structures employing vibration-sensitive payload require stringent spacecraft attitude control. Examples may include imaging payloads with rotating or scanning instruments that have high-accuracy pointing and jitter requirements. Control systems are needed that can suppress spacecraft structural vibrations. When the structure is light and flexible, spacecraft with agile maneuver requirements need special attention. Because of the very small structural damping, it is necessary to minimize the excitation of the flexible modes during the large slew maneuver. Application of the time-optimal design of the rigid body spacecraft to the flexible spacecraft will result in a large excitation of these flexible modes. It is recommended that smoothed feedforward control profiles and trajectory tracking can significantly reduce the maneuver time and settling time.¹ The smooth control profile will eliminate the infinite jerk from each step of the time-optimal bang-bang control. However, smoothing of the control profile cannot completely eliminate the vibration. For a complete cancellation of the vibration, the input shaping technique³ has been successfully adopted and tested with the experimental testbed for rest-to-rest maneuvers.⁶ Input shaping can be used in conjunction with any reference input. When time-optimal bang-bang control is used as a reference control input, the resulting control will completely eliminate the targeted frequency vibration mode. However, the resulting shaped control profile will still have infinite jerk which may result in excitation of the unmodelled dynamics of the system. Therefore, a smooth reference control profile is still preferable for input shaping. The shaped control profile is no longer time-optimal since the final time has been increased by the half period of the each targeted frequency. For systems with multiple frequency modes (especially low frequency modes), sequential application of the input shapers unnecessarily reduce the control amplitude and increase the final time significantly. This fact can be overcome by including the flexible dynamics of the system into the spacecraft model. Then the time-optimal control profile including the flexible modes can be found. Since the resulting time-optimal control is still a bang-bang type with increased switch times, the jerk-limited time-optimal control has been also proposed.⁴ The infinite jerk profile of the step is modified with the ramp input with a constrained maximum jerk value. This method is advantages over the sequential input shaping method in reducing the final time, however, problem solving requires numerical or parameter optimization once the flexible dynamics are included in the model.

In this paper, various aforementioned control profiles are derived for actual implementation on the experimental testbed. The detailed procedure of deriving the various control profiles is also presented. Ex-

*NRC Research Associate, Department of Mechanical and Astronautical Engineering, Naval Postgraduate School, Monterey, CA 93943, Member AIAA.

†Distinguished Professor, Department of Mechanical and Astronautical Engineering, Naval Postgraduate School, Monterey, CA 93943, Associate Fellow AIAA.

| Report Documentation Page | | | <i>Form Approved OMB No. 0704-0188</i> | |
|---|------------------------------------|---|---|----------------------------------|
| <p>Public reporting burden for the collection of information is estimated to average 1 hour per response, including the time for reviewing instructions, searching existing data sources, gathering and maintaining the data needed, and completing and reviewing the collection of information. Send comments regarding this burden estimate or any other aspect of this collection of information, including suggestions for reducing this burden, to Washington Headquarters Services, Directorate for Information Operations and Reports, 1215 Jefferson Davis Highway, Suite 1204, Arlington VA 22202-4302. Respondents should be aware that notwithstanding any other provision of law, no person shall be subject to a penalty for failing to comply with a collection of information if it does not display a currently valid OMB control number.</p> | | | | |
| 1. REPORT DATE AUG 2006 | 2. REPORT TYPE | 3. DATES COVERED 00-00-2006 to 00-00-2006 | | |
| 4. TITLE AND SUBTITLE Experiments on Jerk-Limited Slew Maneuvers of a Flexible Spacecraft | | | 5a. CONTRACT NUMBER | |
| | | | 5b. GRANT NUMBER | |
| | | | 5c. PROGRAM ELEMENT NUMBER | |
| 6. AUTHOR(S) | | | 5d. PROJECT NUMBER | |
| | | | 5e. TASK NUMBER | |
| | | | 5f. WORK UNIT NUMBER | |
| 7. PERFORMING ORGANIZATION NAME(S) AND ADDRESS(ES) Naval Postgraduate School, Department of Mechanical and Astronautical Engineering, Monterey, CA, 93943 | | | 8. PERFORMING ORGANIZATION REPORT NUMBER | |
| 9. SPONSORING/MONITORING AGENCY NAME(S) AND ADDRESS(ES) | | | 10. SPONSOR/MONITOR'S ACRONYM(S) | |
| | | | 11. SPONSOR/MONITOR'S REPORT NUMBER(S) | |
| 12. DISTRIBUTION/AVAILABILITY STATEMENT Approved for public release; distribution unlimited | | | | |
| 13. SUPPLEMENTARY NOTES | | | | |
| 14. ABSTRACT | | | | |
| 15. SUBJECT TERMS | | | | |
| 16. SECURITY CLASSIFICATION OF: | | | 17. LIMITATION OF ABSTRACT Same as Report (SAR) | 18. NUMBER OF PAGES 20 |
| a. REPORT unclassified | b. ABSTRACT unclassified | c. THIS PAGE unclassified | 19a. NAME OF RESPONSIBLE PERSON | |

perimental results are also presented to exemplify and test various jerk limited control methods, using the Flexible Spacecraft Simulator (FSS) developed at the Naval Postgraduate School.

II. Overview of Flexible Spacecraft Simulator

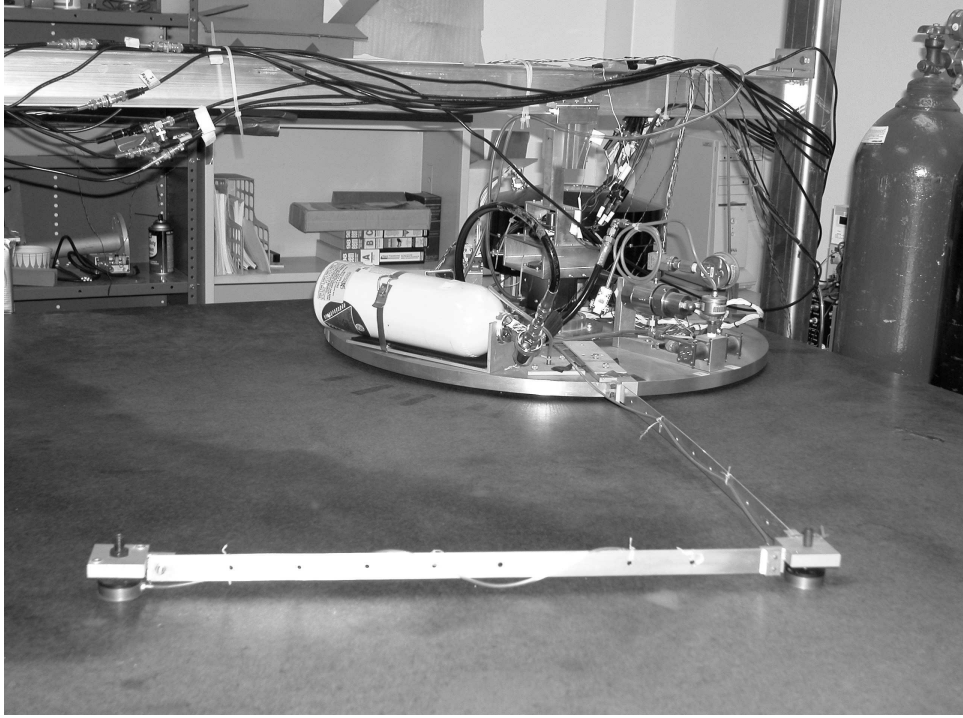


Figure 1. Flexible Spacecraft Simulator (FSS)

The Flexible Spacecraft Simulator (FSS) is designed to study the effect of various control schemes for effective elimination of undesirable vibrations of the flexible body. It is comprised of a rigid hub and a flexible appendage as shown in Figure 1. The flexible appendage is composed of a base beam cantilevered to the rigid hub and a tip beam rigidly connected to the base beam at a right angle. The simulator has one reaction wheel and two cold gas thrusters for the actuation of the rigid hub. The FSS is supported by five air pads on a granite table to simulate a frictionless environment. Angular position of the spacecraft hub is measured by the Rotation Variable Displacement Transducer (RVDT). Angular velocity of the hub is measured by a rate gyro installed on the simulator. An accelerometer is also installed to measure the acceleration of the tip of the flexible appendage. Data acquisition is performed via a dSPACE DS-1103 controller board hosted by a personal computer. The control method is programmed and compiled using Matlab/Simulink and downloaded to the controller board for implementation.

III. Mathematical Model of Flexible Spacecraft Simulator

The equation of motion describing the dynamics of the Flexible Spacecraft Simulator can be written as²

$$\begin{aligned} J_{zz}\ddot{\theta} + \sum_{i=1}^n D_i\ddot{q}_i &= u \\ \ddot{q}_i + 2\zeta_i\omega_i\dot{q}_i + \omega_i^2 q_i + D_i\ddot{\theta} &= 0 \quad (i = 1 \dots n) \end{aligned} \quad (1)$$

where θ is the angular position of the hub, q_i represents for the i^{th} flexible mode, J_{zz} is the moment of inertia of the whole system, u is the total torque applied to the main body, ζ_i is the damping ratio of the i^{th} flexible mode, and ω_i is the natural frequency of the i^{th} flexible mode. The rigid-elastic coupling for the

i^{th} flexible mode, D_i , is given by

$$D_i = \int_F (x_F \phi_i^y - y_F \phi_i^x) dm \quad (2)$$

where x_F and y_F are coordinates of a point on the flexible structure, and ϕ_i^x and ϕ_i^y are the x and y component of the i^{th} modal vector respectively. The equation of motion can be written as a set of second order differential equations such that

$$\begin{bmatrix} J_{zz} & D^T \\ D & I \end{bmatrix} \begin{bmatrix} \ddot{\theta} \\ \ddot{\mathbf{q}} \end{bmatrix} + \begin{bmatrix} 0 & 0 \\ 0 & \Gamma_c \end{bmatrix} \begin{bmatrix} \theta \\ \mathbf{q} \end{bmatrix} + \begin{bmatrix} 0 & 0 \\ 0 & \Lambda_c \end{bmatrix} \begin{bmatrix} \theta \\ \mathbf{q} \end{bmatrix} = \begin{bmatrix} 1 \\ 0 \end{bmatrix} u \implies M\ddot{\mathbf{z}} + C\dot{\mathbf{z}} + K\mathbf{z} = \mathbf{b}u \quad (3)$$

where

$$\Gamma_c = \begin{bmatrix} 2\zeta_1\omega_1 & 0 & \cdots & 0 \\ 0 & 2\zeta_2\omega_2 & \cdots & 0 \\ 0 & 0 & \ddots & 0 \\ 0 & 0 & 0 & 2\zeta_n\omega_n \end{bmatrix}, \quad \Lambda_c = \begin{bmatrix} \omega_1^2 & 0 & \cdots & 0 \\ 0 & \omega_2^2 & \cdots & 0 \\ 0 & 0 & \ddots & 0 \\ 0 & 0 & 0 & \omega_n^2 \end{bmatrix} \quad \text{and} \quad D = \begin{bmatrix} D_1 \\ D_2 \\ \vdots \\ D_n \end{bmatrix} \quad (4)$$

Assuming that the matrix C is a linear combination of M and K , the equation of motion can be decoupled into a rigid body mode and n set of flexible modes. Define the new decoupled states η as $\mathbf{z} = V\eta$, where columns of V is the eigenvectors of $M^{-1}K$. Then, the decoupled state equation of motion becomes

$$\ddot{\eta} + V^{-1}M^{-1}CV\dot{\eta} + V^{-1}M^{-1}KV\eta = V^{-1}M^{-1}\mathbf{b}u \implies \ddot{\eta} + \Gamma\dot{\eta} + \Lambda\eta = \gamma u \quad (5)$$

The matrices, Γ and Λ , are now diagonal. The equation of motion is further represented by a state-space form as

$$\dot{\mathbf{x}} = A\mathbf{x} + Bu \quad (6)$$

where

$$\begin{aligned} \mathbf{x} &= \begin{bmatrix} \eta_0 & \eta_1 & \cdots & \eta_n & \dot{\eta}_0 & \dot{\eta}_1 & \cdots & \dot{\eta}_n \end{bmatrix} \\ A &= \begin{bmatrix} 0 & I \\ -\Lambda & -\Gamma \end{bmatrix} \quad B = \begin{bmatrix} 0 \\ \gamma \end{bmatrix} \end{aligned} \quad (7)$$

States are defined such that η_0 represents rigid body mode and $\eta_1 \cdots \eta_n$ represent n flexible modes.

IV. Control Design of Flexible Spacecraft Simulator

A. Jerk Limited Control of a Rigid Body

1. Bang-Bang Control

The simplest approach to design a control input for slew maneuvers is to consider only the rigid body mode of the system and design a time-optimal control. From the decoupled equation of motion in Equation 5, the rigid body mode equation of motion can be extracted as

$$\ddot{\eta}_0 = \gamma_0 u \quad (8)$$

The resulting time-optimal rest-to-rest maneuver control profile for the rigid body equation is a bang-bang with one switch at the mid-maneuver time. The total maneuver time is determined to satisfy the boundary condition of the maneuver (i.e. initial and final displacement). The solution to the rigid body equation is one switch bang-bang with one switch at $0.5T_f$, where the final time T_f is

$$T_f = \sqrt{\frac{4d}{\gamma_0 u_{\max}}} \quad (9)$$

where d is the desired rigid body displacement. The optimality of the control can be easily verified by formulating Hamiltonian and investigating the co-states and the switching curve. The time-optimal Bang-Bang control profile has to be modified if there is a saturation of the control torque from the reaction wheel.

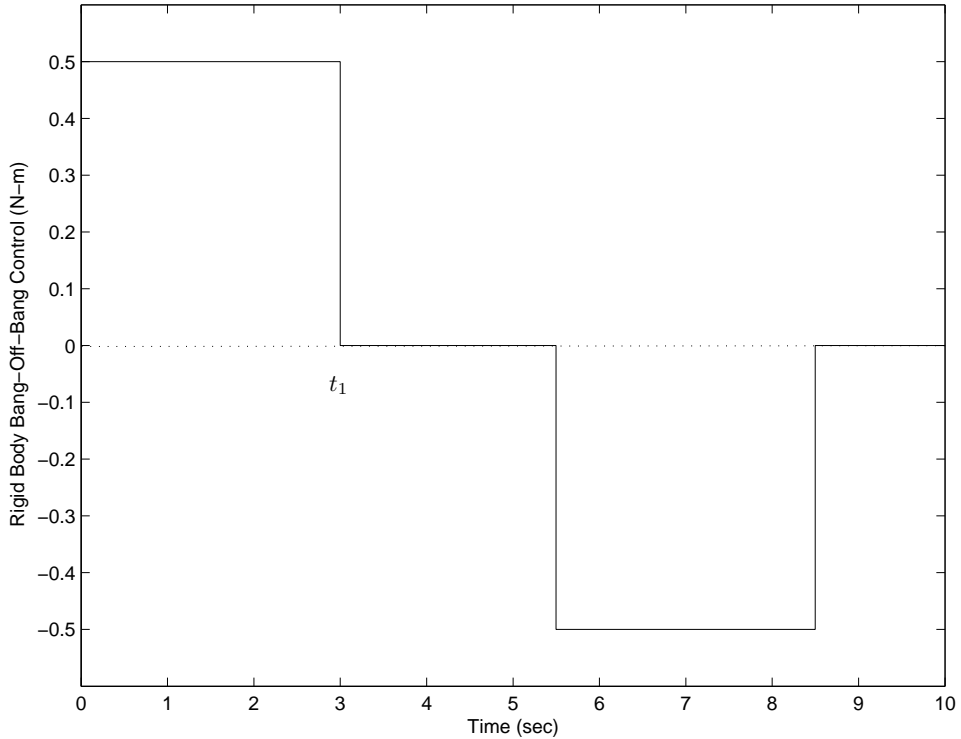


Figure 2. Rigid Body Bang-Off-Bang Control Input

Since there is a limitation of the maximum speed of the reaction wheel, the control needs to be turned off at the saturation limit. The time when the reaction wheel reaches its maximum velocity becomes

$$t_1 = \frac{J_w \max(\dot{\theta}_w)}{u_{\max}} \quad (10)$$

where, J_w is inertia of reaction wheel, $\dot{\theta}_w$ is the angular velocity of reaction wheel, and u_{\max} is maximum torque such that

$$u_{\max} = \frac{\max(\ddot{\theta}_w)}{J_w} \quad (11)$$

where $\ddot{\theta}_w$ is the maximum acceleration of the reaction wheel. Figure 2 illustrates the rigid body bang-off-bang control profile. Jerk is defined as a rate of change of control. Jerk becomes the energy transmitted to excite the flexible modes of the system. From the rigid body bang-off-bang control profile, the control will change its value instantaneously at the control switches, which will result in an infinite jerk. This will create undesirable vibration if the bang-off-bang control is used in the flexible system. Limiting this infinite jerk is discussed in the following sections.

2. Use of Known Smooth Curves for Jerk Limitation

It is shown in¹ that the simple smooth curve approximation of the bang-bang control profile can be effective in reducing the residual vibration for a slew maneuver. Since the smooth curve has a finite jerk value, each step of the bang-bang control can be approximated with some known smooth curve. In this paper, the versine function⁶ is adopted for a smooth control profile. Figure 3 shows the jerk limited control profile using the versine function. From Figure 3, smooth parameter α is defined such that

$$t_A = \alpha \frac{t_1}{2} \quad 0 \leq \alpha \leq 1 \quad (12)$$

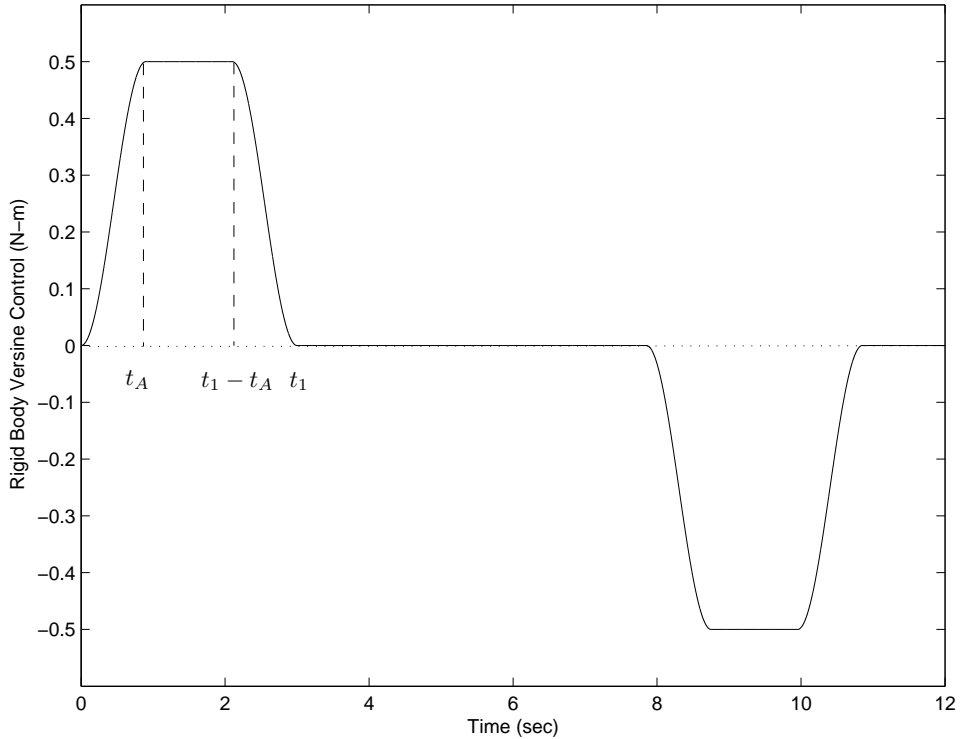


Figure 3. Versine Control Input Profile ($\alpha = 0.6$)

Then, the maximum jerk can be adjusted by the value of α . The versine control input can be written as a function of time as

$$\begin{aligned} u(t) &= 0.5T_{\max} \left(1 - \cos \frac{\pi}{t_A} t \right) & 0 \leq t < t_A \\ u(t) &= T_{\max} & t_A \leq t < t_1 - t_A \\ u(t) &= 0.5T_{\max} \left[1 + \cos \frac{\pi}{2t_A} (t - (t_1 - t_A)) \right] & 0 \leq t < t_A \end{aligned} \quad (13)$$

The deceleration phase, the control profile becomes negative. The maximum jerk in this profile becomes

$$J_{\max} = \frac{u_{\max} \pi}{2t_A} \quad (14)$$

3. Polynomial Approach

Another approach to limit the jerk in the control design is to use the polynomial function instead of a known smooth function. Then the polynomial function can be optimized such that the maximum jerk of the control profile is minimized. This dictates solving the minimax optimization problem. A simplest direct method for this problem is to utilize the linear programming technique. The n^{th} order polynomial control input can be written as

$$u(t) = \mathbf{T}\mathbf{a} \quad (15)$$

where $\mathbf{T} = [t^0 \ t^1 \ t^2 \ \dots \ t^n]$ and $\mathbf{a} = [a_0 \ a_1 \ a_2 \ \dots \ a_n]^T$. Now \mathbf{a} is the vector of unknown coefficients of polynomial function. The jerk at time t is now written as

$$\dot{u}(t) = \frac{d\mathbf{T}}{dt} \mathbf{a} \quad (16)$$

For a polynomial control profile rising from 0 to T_{\max} with given time t_A and maximum jerk J_{\max} , the linear programming problem statement becomes

$$\begin{aligned}
 \text{find } \mathbf{a} &= [a_0 \ a_1 \ a_2 \cdots a_n]^T \\
 \text{subject to the constraints} \\
 u(0) &= 0, \quad \dot{u}(0) = 0 \\
 u(t_A) &= T_{\max}, \quad \dot{u}(t_A) = 0 \\
 |\dot{u}(t_i)| &= \left| \frac{d\mathbf{T}}{dt} \Big|_{t=t_i} \mathbf{a} \right| \leq J_{\max}, \quad (0 \leq t_i \leq t_A)
 \end{aligned} \tag{17}$$

The inequality condition requires discretization of time t_i between $t = 0$ and $t = t_A$. Note that the additional

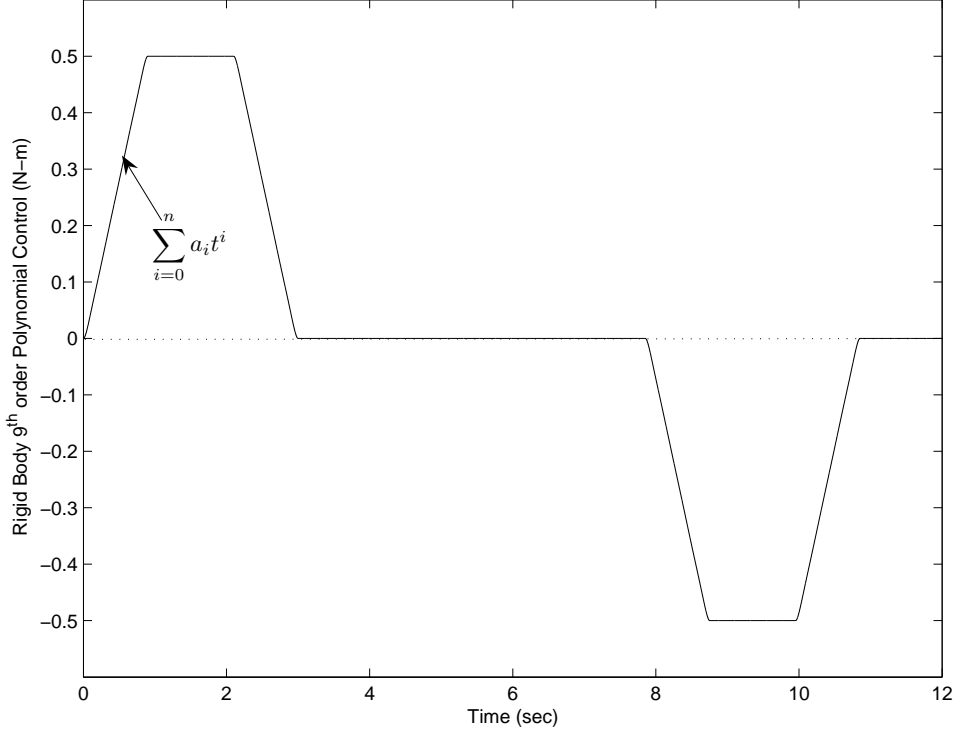


Figure 4. n^{th} Order Polynomial Control Input Profile ($\alpha = 0.6$, $n = 9$)

constraints of $\dot{u}(0) = 0$ and $\dot{u}(t_A) = 0$ are added to smooth the control at the beginning and at the end of the control profile. Further smoothing can be possible by adding more constraints, for example $\ddot{u}(0) = 0$ and $\ddot{u}(t_A) = 0$. The smoothness of the control profile can also be modified by utilizing a different order of polynomial functions. This linear programming formulation is a phase 1 problem in order to find the coefficient satisfying constraints with given maximum jerk J_{\max} and time t_A . If the solution to the problem is feasible, the maximum jerk can be reduced further until the feasible solution is not found. Then the jerk value becomes the minimum of maximum jerk within the given time $[0 \quad t_A]$. Similar problems can also be solved while fixing the maximum jerk value and minimizing the time t_A . For efficient reduction in J_{\max} or t_A , the bisection algorithm can also be used. With the approach used in the previous optimization technique, the 9th order polynomial profile control profile can be obtained for rigid body spacecraft model as shown in Figure 4.

4. Effect of Jerk Limitation

In the previous sections, the method of jerk limitation has been presented. In order to study the effect of jerk, simple second order mass-spring system of $\ddot{x} + 2\zeta\omega_n\dot{x} + \omega_n^2 x = \omega_n^2 u$ is considered with the input profiles designed in the previous section as shown in Figure 5. The control rise time, t_A , determines the maximum jerk of the input profiles and the amplitude of the control after time t_A is designed to be 1. The residual

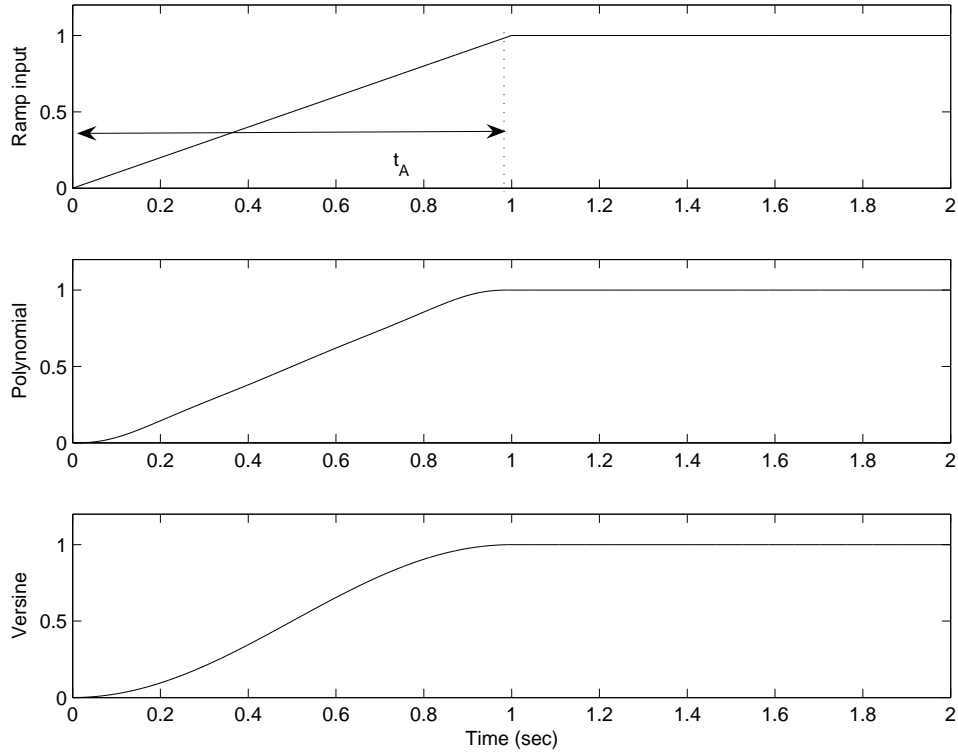


Figure 5. Jerk Limited Input Profiles

energy at time t_A due to the flexibility of the system can be written as

$$E(t_A) = \sqrt{\frac{1}{2}\omega_n^2(x(t_A) - 1)^2 + \frac{1}{2}\dot{x}(t_A)^2} \quad (18)$$

Figure 6 shows how the jerk limitation affects the residual vibration of the different frequency. The ramp input in the top of Figure 5 without damping is used to generate the plot. When $t_A = 0$, the control input becomes a step input and the energy level is large. As t_A increases, the residual energy reduces. With the ramp input with zero damping, the residual energy becomes zero at $t_A = \frac{2n\pi}{\omega_n}$ with the positive integer n . Therefore, there are no advantages of increasing t_A beyond $\frac{2\pi}{\omega_n}$. Also, it can be seen that the energy rolls off more quickly for higher frequencies than for low frequencies. Figure 7 shows how the residual energy changes with different control profiles and damping values. From the top plot of Figure 7, residual energy reduction is slower for polynomial and versine profile since the maximum jerk is higher than the ramp input for the same control rise time. For the practical application of reference trajectory tracking of a spacecraft, a smoothed control profile is more advantageous because of the resulting smoother reference trajectory. With the presence of damping, the residual energy cannot reach zero with the jerk limitation as shown in second and third plots of Figure 7. With the increased damping of $\zeta = 0.5$, the versine profile was able to reduce the residual energy more for given control rise time.

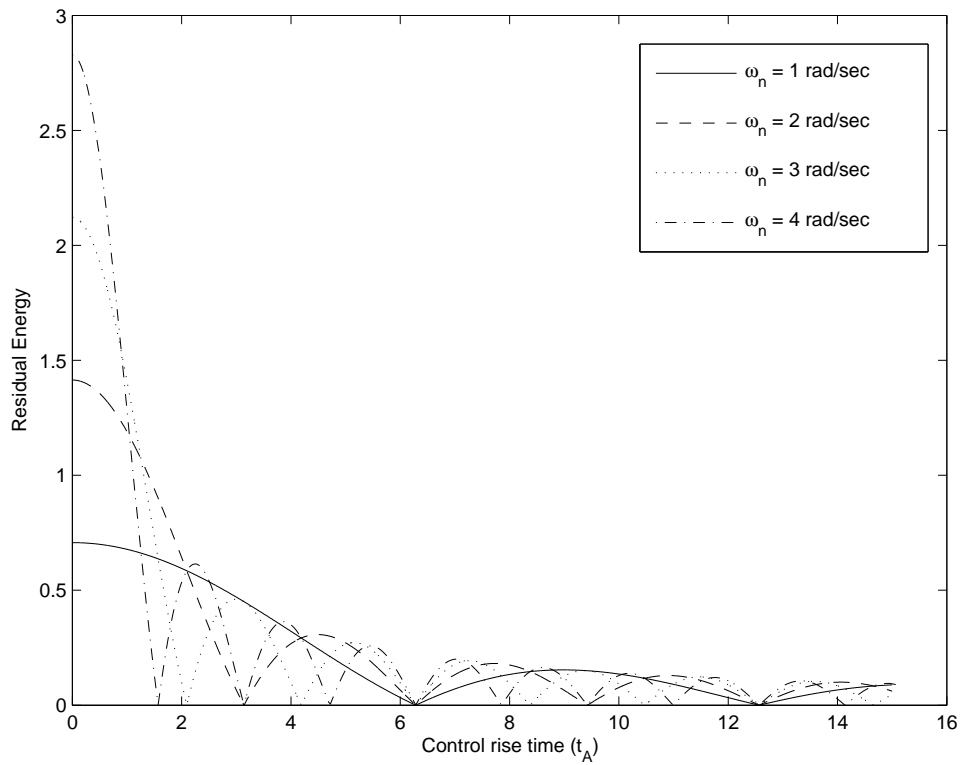


Figure 6. Residual Energy for Different Frequencies (Ramp Input without Damping)

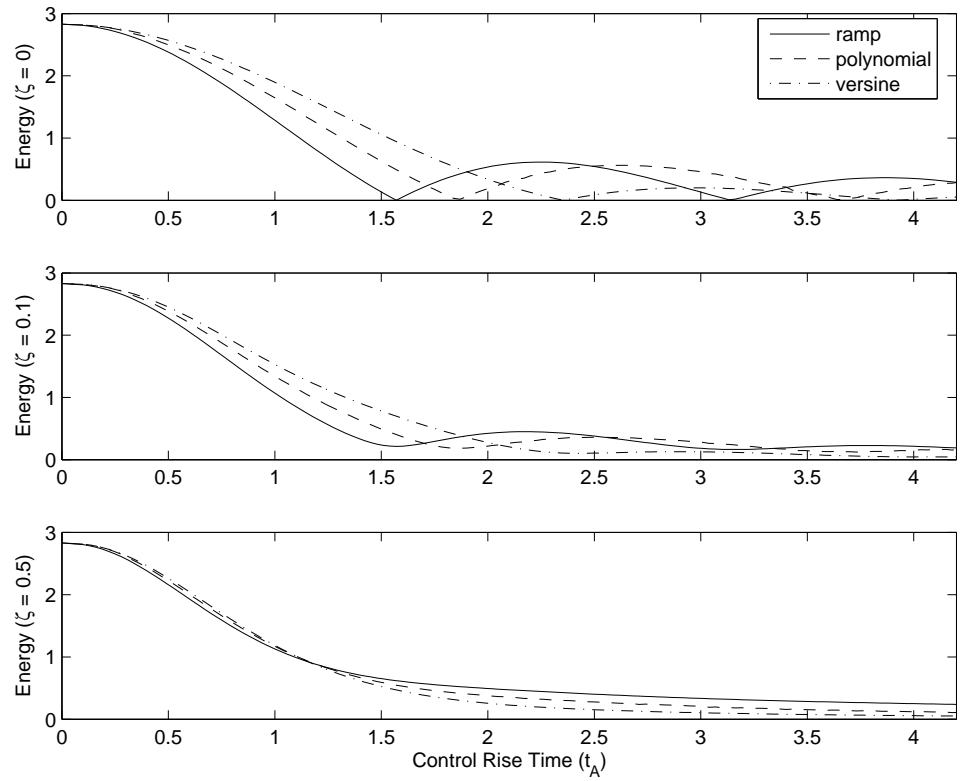


Figure 7. Residual Energy for Different Control Profiles and Damping Ratios ($\omega_n = 4\text{rad/sec}$)

5. Simulation Results of Jerk Limited Rigid Body Control Profiles

From the analysis given in,² the mathematical model with one rigid body mode and eight flexible modes under 100 Hz is utilized for numerical simulation. Parameters of the Flexible Spacecraft Simulator for Equation 3 are

$$\begin{aligned} J_{zz} &= 7.874 \text{ Kg} \cdot m^2 \\ D &= \begin{bmatrix} -0.9334 & -0.6018 & -0.0463 & -0.0545 & -0.0306 & -0.0273 & -0.0195 & -0.0113 \end{bmatrix}^T \\ \Lambda_c &= \text{diag}(2\pi[0.2510 \ 0.7084 \ 9.369 \ 16.15 \ 34.70 \ 46.81 \ 77.00 \ 94.83]) \end{aligned} \quad (19)$$

The simulation was performed with the maximum torque of $u_{\max} = 0.5 \text{ N}\cdot\text{m}$ and desired slew angle of $d = 60$ degrees. 5 percent damping is added to the each flexible mode for simulation. The control turn-off time, t_1 , was set to be 3 sec and the final maneuver time was determined to satisfy the displacement constraint. With

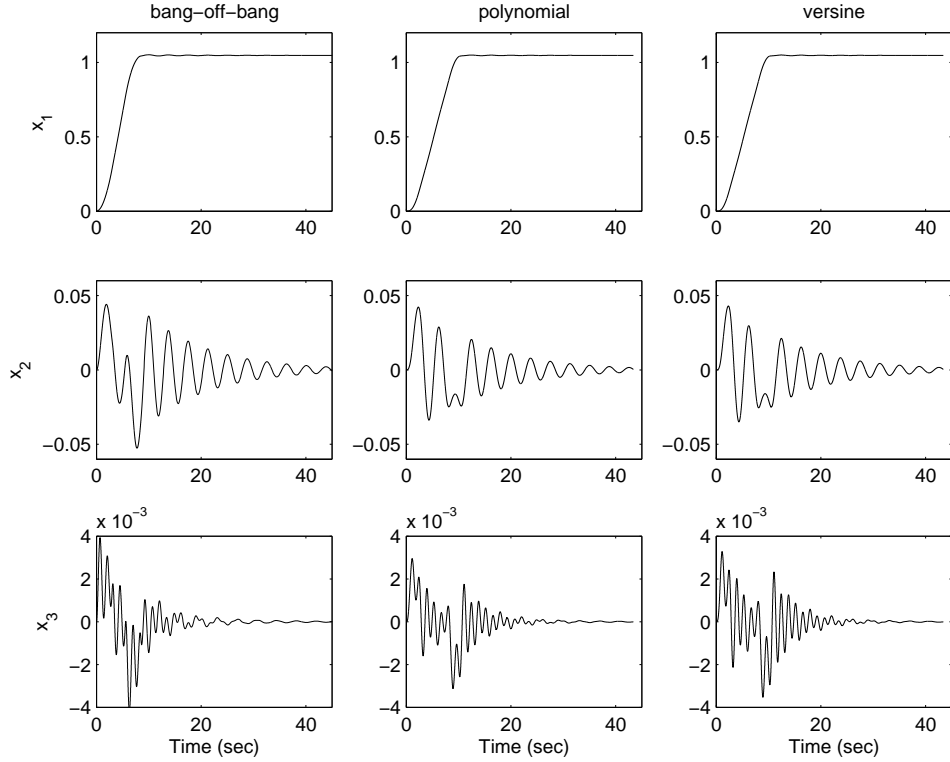


Figure 8. Response first three states including hub rotation

the feedforward application of the three different control profiles (bang-off-bang, polynomial, and versine), responses of the first six states including the spacecraft hub rotation are plotted in Figure 8 and Figure 9. If the flexible modes were not excited with these control profiles, there would be no residual vibration and the steady-state error at the end of the maneuver would be zero. However, excitation of the flexible modes of the system results in undesirable residual vibration and maneuver displacement error. The response plots show that the flexible modes are less excited for polynomial and versine control profiles than bang-off-bang control profile due to the limitation in jerk. The states with higher frequency contents in Figure 9 show that the high frequency modes are minimally excited for polynomial and versine control profiles, although quickly damped out for the bang-bang control profile. Therefore, low frequency mode excitation more significantly effects the spacecraft hub vibration. Figure 10 shows the spacecraft hub displacement at the end of the maneuver. The bang-off-bang profile has the smallest control final time, however, it yields a largest residual vibration. With the jerk limitation with versine and polynomial control profile, the residual vibration is reduced. The residual vibration can be further reduced by increasing the control rise time, however, the control actuation time will be significantly increased for low frequency modes. Therefore, the control profile should be designed to minimize the low frequency vibration in a more effective manner.

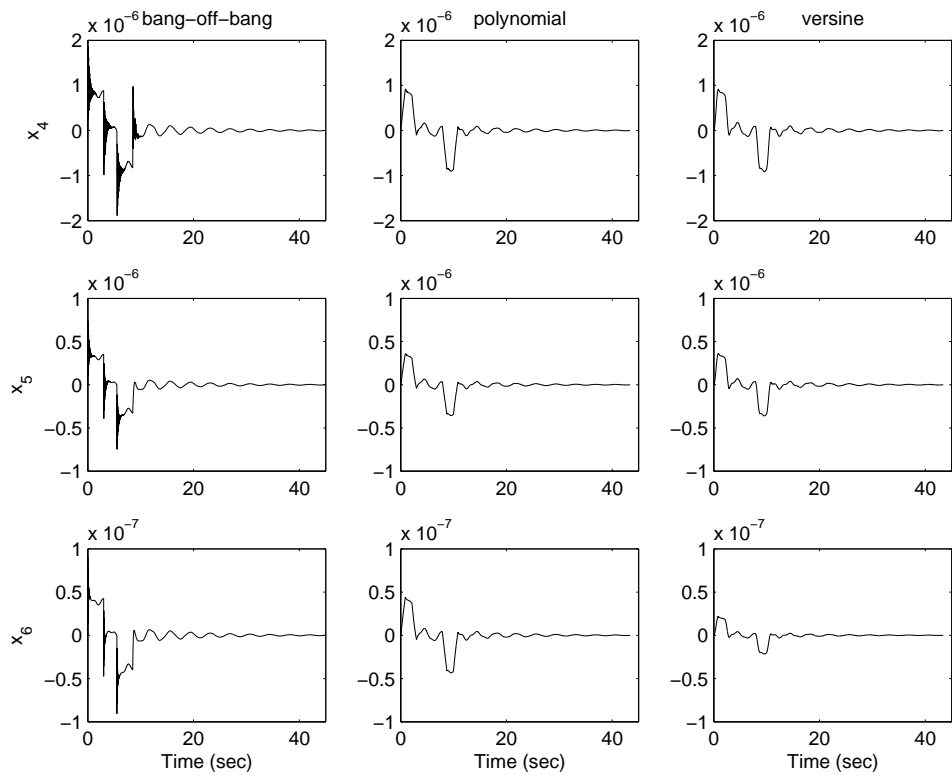


Figure 9. Response of states with higher frequency contents

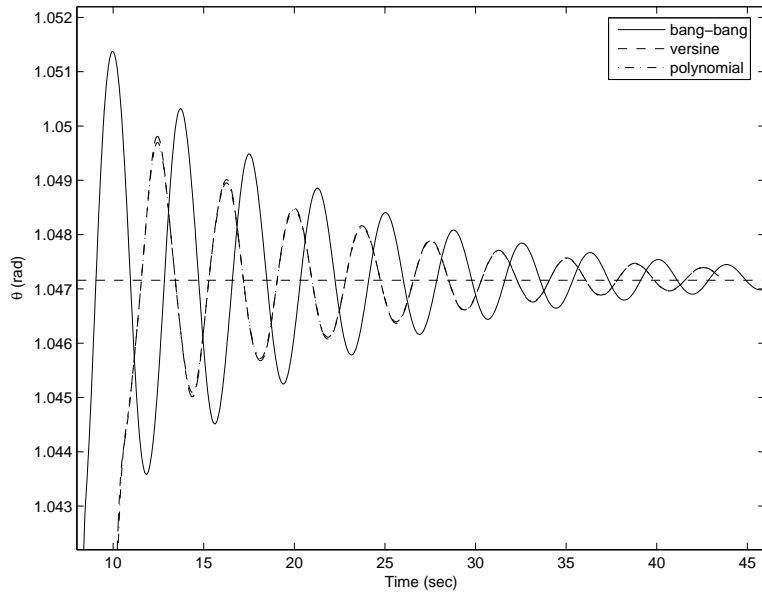


Figure 10. Position Error of Spacecraft Hub

B. Control Design for Low Frequency Modes

1. Input Shaping

With the jerk limitation of the rigid body control profile, excitation of the flexible modes can be reduced. With the of single rigid body mode and single flexible mode with no damping, the vibration can be completely eliminated with the proper selection of control rise time. However, this will require that each step of the bang-bang control should be approximated with a smooth control profile with the minimum control rise time of $\frac{2\pi}{\omega_n}$, depending on the jerk limitation method. Input shaping is an effective method to cancel the flexible dynamics of the system, which can be well suited for cancelling the low frequency mode excitation effect.³ The input shaping technique requires the control input to be convoluted with a set of impulses such that the resulting control input cancels out the flexible dynamics of the system. Since we are targeting the low frequency modes of the system, two low frequency modes of the Flexible Spacecraft Simulator are considered. The decoupled equation of motion considering only two dominant flexible modes is

$$\begin{bmatrix} \ddot{\eta}_0 \\ \ddot{\eta}_1 \\ \ddot{\eta}_2 \end{bmatrix} + \begin{bmatrix} 0 & 0 & 0 \\ 0 & 2.794 & 0 \\ 0 & 0 & 20.911 \end{bmatrix} \begin{bmatrix} \eta_0 \\ \eta_1 \\ \eta_2 \end{bmatrix} = \begin{bmatrix} 0.127 \\ -0.133 \\ -0.093 \end{bmatrix} u \quad (20)$$

The eigenvalues of the system are 0, 2.794, and 20.911, respectively. The rigid body mode corresponds to 0 eigenvalue, and the frequency of two flexible modes are defined such that $\omega_1^2 = 2.794$ and $\omega_2^2 = 20.911$. For the zero vibration input shaping technique with specific target frequency, the impulse sequence is defined as

$$A_i = \left[\frac{e^{\frac{\zeta\pi}{\sqrt{1-\zeta^2}}}}{1 + e^{\frac{\zeta\pi}{\sqrt{1-\zeta^2}}}} \quad \frac{1}{1 + e^{\frac{\zeta\pi}{\sqrt{1-\zeta^2}}}} \right], \quad t_i = [0 \quad \frac{\pi}{\omega\sqrt{1-\zeta^2}}] \quad (21)$$

where A_i denotes the amplitude of the impulse and t_i denotes the time when the corresponding magnitude of A_i impulse is applied. The input shaping technique can handle multiple frequencies by convolving multiple impulse sequences. The shaped control profile will have an added control time of half the damped period for each targeted frequency mode. Figure 11 shows the shaped control with 9th order polynomial input targeting two low frequency modes of the system. The maneuver time has increased by one half period of each flexible mode frequency compared to the reference polynomial input. Since the reference input has a limited jerk, the resulting shaped input also has a limited jerk value. Since the positive impulse sequence is used and the sum of the impulses are 1, the resulting shaped control is guaranteed to have a maximum jerk less than or equal to the maximum jerk of the reference control input.

2. Jerk Limited Optimal Control Including Dominant Flexible Modes

In designing a slew maneuver control, one natural choice is to find a minimum-time solution for fast pointing. Using the input shaping method with positive impulses, the control level is always less than the maximum torque. The shaped control profile is not time optimal, since the resulting control profile does not utilize maximum torque available. For example, maximum torque used in the shaped input in Figure 11 is less than 0.5 N-m, which is the maximum torque limit. Therefore, it is possible to reduce the final time by find the time-optimal solution that includes the dominant flexible modes from the beginning. Muenchhof and Singh⁴ proposed the time-optimal control profile by modifying the each step of the control with a ramp input, which has a limited jerk value. For a rest-to-rest slew maneuver with rigid body and flexible body modes, the optimal control problem becomes a two point boundary value problem. For a rest-to-rest time-optimal control problem with the given torque constraints, the optimal control profile for systems like Flexible Spacecraft Simulator is a type of bang-bang. If there is no damping, the bang-bang control profile will have $2n+1$ switches, where n is the number of flexible modes. With this knowledge, two point boundary problem can be solved with parameter optimization where the unknown parameters are the switch and final time. The constraints for the parameter optimization are obtained from the input shaping⁵ or time-delay filter technique,⁴ because the vibration of the flexible mode has to be zero at the end of the maneuver. An additional constraint is the boundary condition to meet the displacement requirement. For a system given in Equation 20, the time-optimal control input is 5 switch bang-bang. With the input shaping technique,

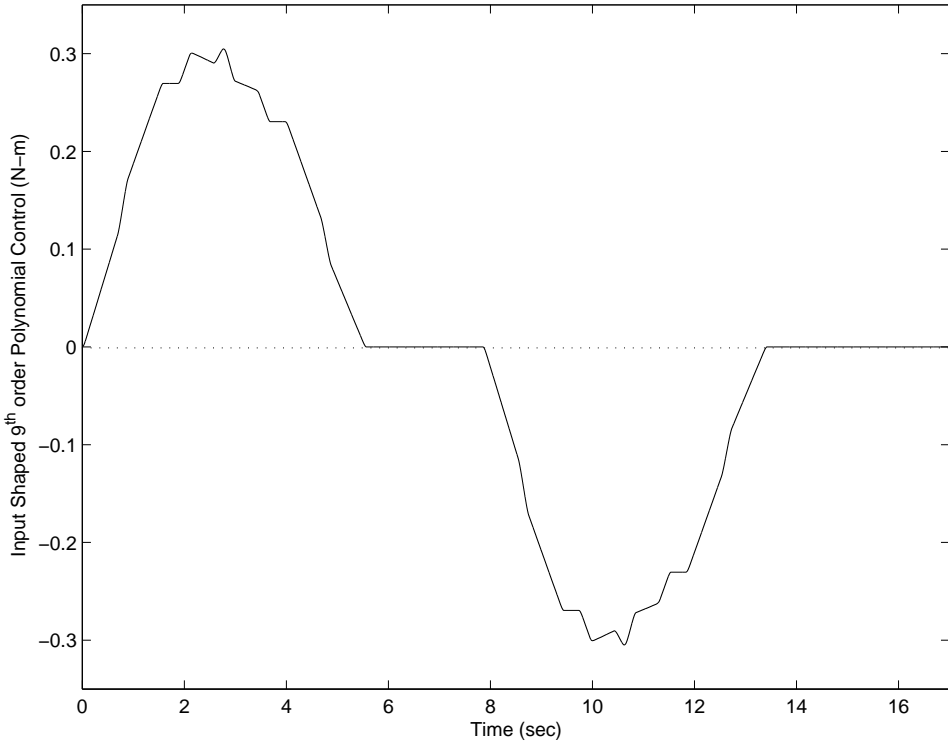


Figure 11. Shaped 9th Order Polynomial Control Input

the step size of maximum control torque of u_m is shaped with a set of impulses, which are defined by

$$\begin{aligned} A_i &= \begin{bmatrix} 1 & -2 & 2 & -2 & 2 & -2 & 1 \end{bmatrix} \\ t_i &= \begin{bmatrix} 0 & T_1 & T_2 & T_3 & T_4 & T_5 & T_6 \end{bmatrix} \end{aligned} \quad (22)$$

where, $T_1 \cdots T_5$ is switch times and T_6 is the final time. The resulting shaped control profile is 5 switch bang-bang with unknown switch and final time. It is same as filtering the step input with the step size of u_m with the following time-delay filter in the frequency domain.

$$G(s) = 1 - 2e^{-sT_1} + 2e^{-sT_2} - 2e^{-sT_3} + 2e^{-sT_4} - 2e^{-sT_5} + e^{-sT_6} \quad (23)$$

Now the time-optimal control problem becomes finding the unknown switch and final time, given the constraints of all the vibration modes are zero and rigid body boundary condition is satisfied at the end of the maneuver. It will result in the same constraints either by solving the impulse sequence for zero vibration or by designing a time-delay filter using frequency domain pole-zero cancellation. Since it is simpler to derive constraints in the frequency domain, pole-zero cancellation approach is used with the time-delay filter. The system has two poles at 0, two conjugate poles at $\pm j1.6715$, and two conjugate poles at $\pm j4.5729$. From the pole-zero cancellation, the constraints for parameter optimization become

$$G(s)|_{s=0} = 0 \quad \left. \frac{dG(s)}{ds} \right|_{s=0} = 0 \quad G(s)|_{s=\pm j1.6715} = 0 \quad G(s)|_{s=\pm j4.5729} = 0 \quad (24)$$

One additional constraint is from the boundary conditions. At the initial and final time, the boundary condition is

$$\begin{aligned} \mathbf{z}(t=0) &= [0 \quad 0 \quad 0]^T \\ \mathbf{z}(t=T_6) &= [d \quad 0 \quad 0]^T \end{aligned} \quad (25)$$

The corresponding boundary condition for decoupled states are

$$\begin{aligned} \eta(t=0) &= V^{-1} \mathbf{z}(t=0) \\ \eta(t=T_6) &= V^{-1} \mathbf{z}(t=T_6) \end{aligned} \quad (26)$$

Figure 12 shows the resulting time-optimal control input, which is 5 switch bang-bang. By modifying the

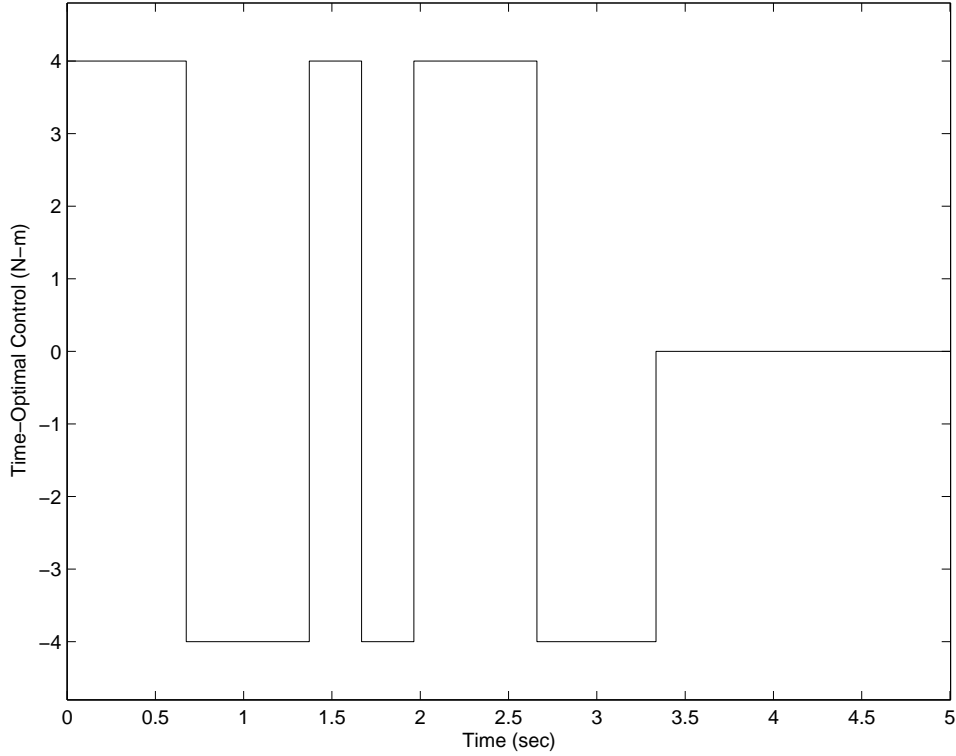


Figure 12. Time-Optimal Control Input of FSS

infinite jerk step of the time-optimal control profile shown in Figure 12, jerk can be limited to reduce the unwanted excitation of the un-modelled frequency modes. In order to do this, define control input u as a state variable such that $\dot{u} = v$. Now v represents jerk and acts as an input variable to the system. From Equation 20, the state-space representation of the system including u state becomes

$$\begin{bmatrix} \dot{\eta} \\ \ddot{\eta} \\ \dot{u} \end{bmatrix} = \begin{bmatrix} 0_{3 \times 3} & I_{3 \times 3} & 0_{3 \times 1} \\ F & 0_{3 \times 3} & G \\ 0_{1 \times 3} & 0_{1 \times 3} & 0_{1 \times 1} \end{bmatrix} \begin{bmatrix} \eta \\ \dot{\eta} \\ u \end{bmatrix} + \begin{bmatrix} 0_{3 \times 1} \\ 0_{3 \times 1} \\ I_{1 \times 1} \end{bmatrix} v \quad (27)$$

Instead of actual control input u , jerk profile is parameterized, which is a bang-off-bang control profile as in the bottom of Figure 13. With this jerk profile, the actual control input will have a limited jerk defined by the maximum value of jerk. Defining maximum jerk and maximum control torque as J_{\max} and u_{\max} , the time-delay filter becomes

$$G(s) = 1 - e^{-s\tau} - e^{-s(T_1-\tau)} + e^{-s(T_1+\tau)} + e^{-s(T_2-\tau)} - e^{-s(T_2+\tau)} - e^{-s(T_3-\tau)} \\ + e^{-s(T_3+\tau)} + e^{-s(T_4-\tau)} - e^{-s(T_4+\tau)} - e^{-s(T_5-\tau)} + e^{-s(T_5+\tau)} + e^{-s(T_6-\tau)} - e^{-sT_6} \quad (28)$$

where, $\tau = \frac{u_{\max}}{J_{\max}}$. From Equation 27, the system has seven poles, where three poles at 0, two conjugate poles at $\pm j1.6715$, and two conjugate poles at $\pm j4.5729$. The constraints for solving unknown switch times and final time are

$$G(s)|_{s=0} = 0 \quad \frac{dG(s)}{ds}\Big|_{s=0} = 0 \quad \frac{d^2G(s)}{ds^2}\Big|_{s=0} = 0 \quad G(s)|_{s=\pm j1.6715} = 0 \quad G(s)|_{s=\pm j4.5729} = 0 \quad (29)$$

With these constraints, parameter optimization was performed with the slew maneuver angle of 0.5 rad, maximum control torque of 4 N-m, and maximum jerk of 30 N-m/sec. The resulting jerk and control profile is shown in Figure 13. It has a slightly larger final maneuver time compared to time-optimal control profile, however, the jerk value has been limited.

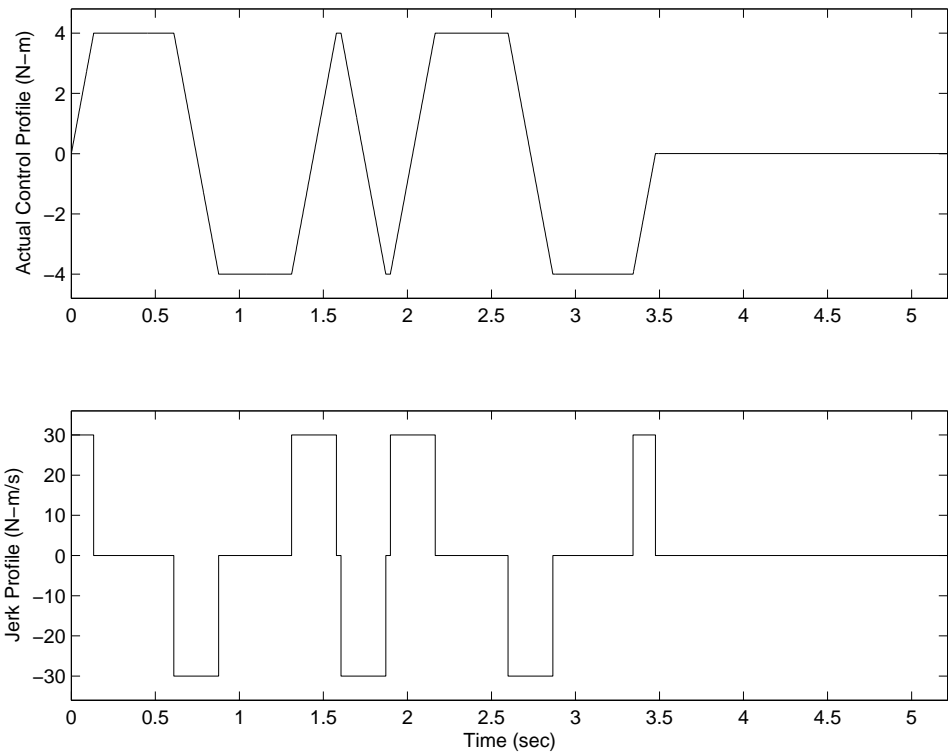


Figure 13. Time-Optimal Control Input of FSS

V. Experiment with Flexible Spacecraft Simulator

A. System Identification of Flexible Spacecraft Simulator

Considering no disturbance to the system, equation of motion of the Flexible Spacecraft Simulator can be rewritten as

$$\begin{aligned} (J_h + J_w)\dot{\omega}_h + \sum_{i=1}^n D_i \ddot{q}_i &= -J_w \dot{\omega}_w = u \\ \ddot{q}_i + 2\zeta_i \omega_i \dot{q}_i + \omega_i^2 q_i + D_i \ddot{\theta} &= 0 \quad (i = 1 \dots n) \end{aligned} \quad (30)$$

From Equation 30, the input of the system becomes the momentum change of the reaction wheel. Therefore, reaction wheel dynamics were first identified. The equation of motion for the reaction wheel ignoring the dynamics of the electrical system of the motor can be written as

$$J_w \dot{\omega}_w + c \omega_w + f_c \text{sign}(\omega_w) = u_v \quad (31)$$

where, J_w is a inertia of the reaction wheel, c is viscous damping coefficient, f_c is coulomb friction, and u_v is the voltage input to the reaction wheel. The angular velocity of the reaction wheel is measured from the hall sensor output. From Figure 14, biased bang-bang control input was used to identified the parameters of the system so that the resulting model closely follow the measured reaction wheel speed response. The bottom of Figure 14 shows the responses of identification result ($J = 0.58$, $c = 0.006$, and $f_c = 0.07$). From

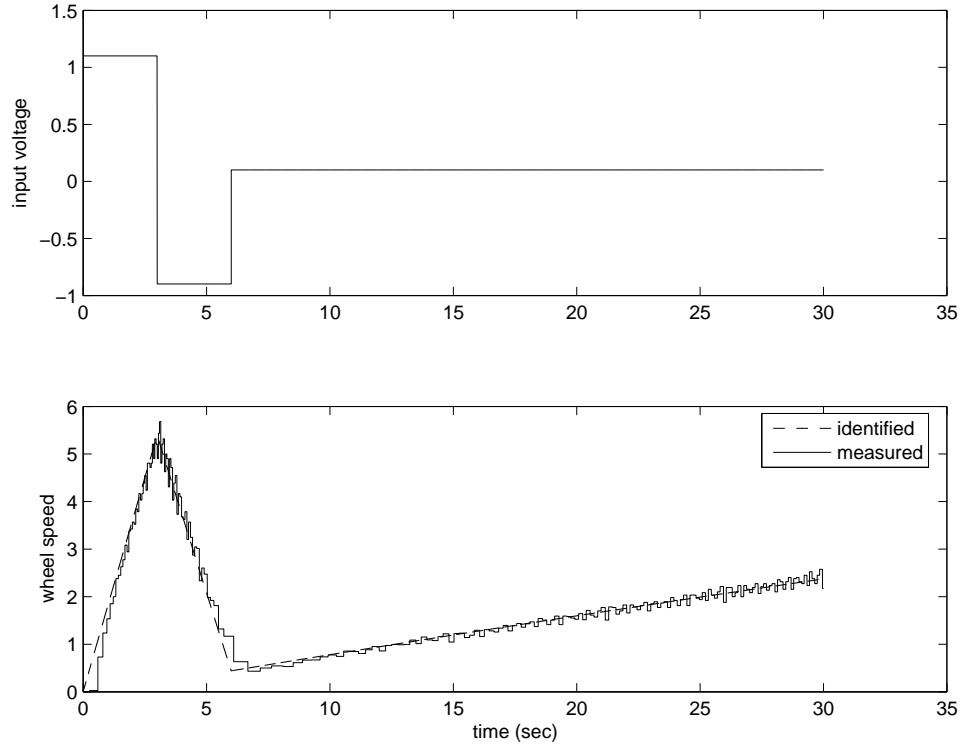


Figure 14. Measured and Identified Reaction Wheel Responses

Equations 30 and 31, the actual control input becomes

$$u = -u_v + c \omega_w + f_c \text{sign}(\omega_w) \quad (32)$$

The actual control input compensates the friction and viscous damping of the reaction wheel such that $J_w \dot{\omega}_w = u_v$. The next step is to identify the dynamics of the Flexible Spacecraft Simulator. Bang-bang input and hub angular position and velocity response data was collected from an experiment. For a determination of the unknown parameters, the number of the flexible modes to be included in the model was first determined. Figure 15 shows the tip acceleration from free response and its Fast Fourier Transformation results. There are three dominant frequency modes at 0 Hz, 0.2554 Hz, and 0.7685 Hz. Therefore, one rigid body mode

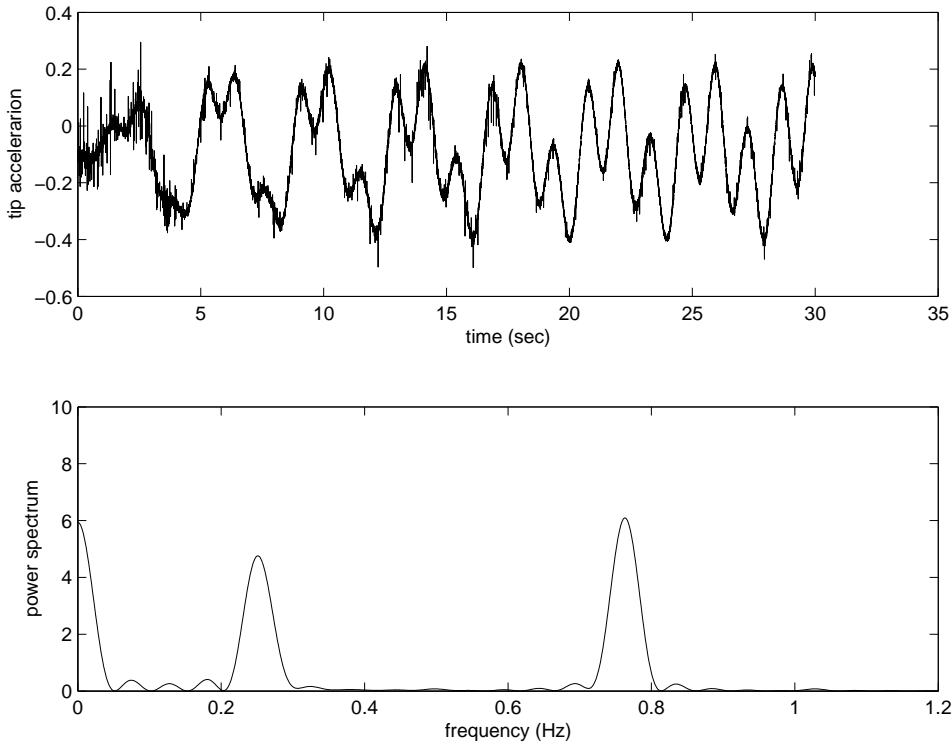


Figure 15. Frequency Contents of FSS

and two flexible body modes are considered. From Equation 30, n becomes 2 and the unknown parameters to be determined are $J_{zz} = J_h + J_w$, d_1 , d_2 , ζ_1 , ζ_2 , ω_1 , and ω_2 . Nonlinear least square optimization was performed to find the unknown parameters which minimizes the cost

$$\sum_{i=1}^{n_d} \left[(\theta(t_i) - \theta_m(t_i))^2 + (\omega(t_i) - \omega_m(t_i))^2 \right] \quad (33)$$

where, n_d is the number of data points, θ and θ_m are angular positions from the model and measurement, and ω and ω_m are angular velocities from the model and measurement. Figure 16 shows the results of the identification with the identified parameters ($J_{zz} = 19.2253$, $d_1 = -1.6190$, $d_2 = -1.1193$, $\omega_1 = 0.2372$ Hz, and $\omega_2 = 0.7435$ Hz). Note that the input is represented by voltage, so torque factor should be multiplied to determine the actual torque in Newtons. From the identified decoupled frequency values of ω_1 and ω_2 , the flexible system frequency becomes 0.2551 Hz and 0.7738 Hz, which are close to the frequencies obtained from the Fast Fourier Transformation in Figure 15.

B. Generation of Reference Trajectory

Feedforward application of the control profile developed in the previous section will always create residual vibration and slew angle error because of incorrect modelling and disturbances. It is more practical to use the tracking type of feedback control law as presented in.¹ This control law is also globally stable about a state at the end of the slew maneuver. Figure 17 shows the control profiles considered in the experiment. They are rigid body time-optimal bang-bang, versine, polynomial, input-shaped polynomial, time-optimal with one rigid body and two dominant flexible modes, and jerk limited time-optimal control profiles. The control profiles are designed for a rest-to-rest maneuver of 0 to 25 degrees. Actuation with maximum/minimim control level of 1.5/-1.5 Volt is limited to 2 seconds to allow the reaction wheel to operate within the maximum angular speed. Smoothing parameter of $\alpha = 0.8$ was used for versine and polynomial control profiles. For a rigid body time-optimal bang-bang and time-optimal with flexible modes have infinite jerk value at the control switches as well as initial and final control time. For a versine profile, the maximum jerk value is 2.9452. For a polynomial control profile, jerk value is minimized to 2.0089. For an input shaped

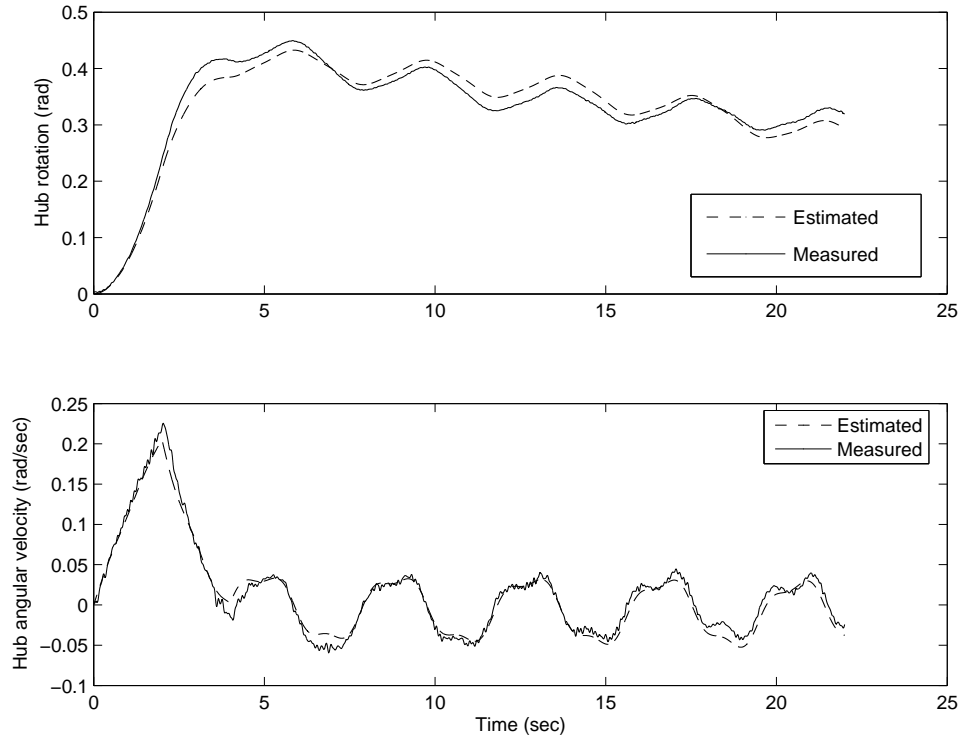


Figure 16. Measured and Identified FSS Hub Responses

polynomial control profile, maximum jerk value is also limited by the jerk value of the polynomial profile. For a jerk limited time-optimal control profile, jerk value is limited to 10 and 2.7. Figure 18 shows the corresponding reference trajectories which are used for the feedback tracking control. Infinite jerk in bang-bang and time-optimal control profiles creates sharp edges on the reference velocity trajectories, whereas jerk limited control profiles have smooth trajectory motion.

C. Experimental Results

With the feedforward control profiles and their corresponding reference trajectories, feedforward and feedback tracking control was performed. Figure 19 shows the resulting trajectory of the spacecraft hub as well as the reference trajectory. It is shown that the resulting trajectory closely follows the reference trajectory. The resulting angular position of the spacecraft hub at the end of the control is also shown in Figure 20. Without end game control at the end of the maneuver, the residual vibration will last a long time. The $3 - \sigma$ bound on angular position error is also shown in the figure. The standard deviation value shows that the smooth control profiles such as versine and polynomial profiles have advantages over bang-off-bang control as expected from.¹ The further improvement can be made with input shaping with the added maneuver time. Since a shaped input has a more smooth control profile, it performed better than time-optimal and jerk limited time-optimal.

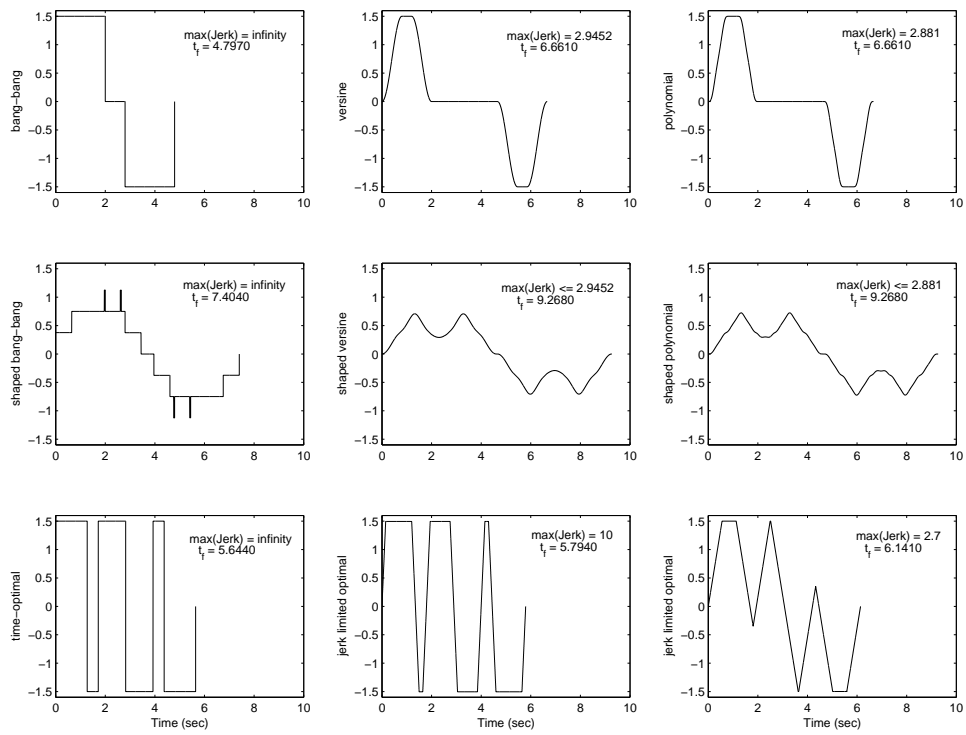


Figure 17. Feedforward Input Profile

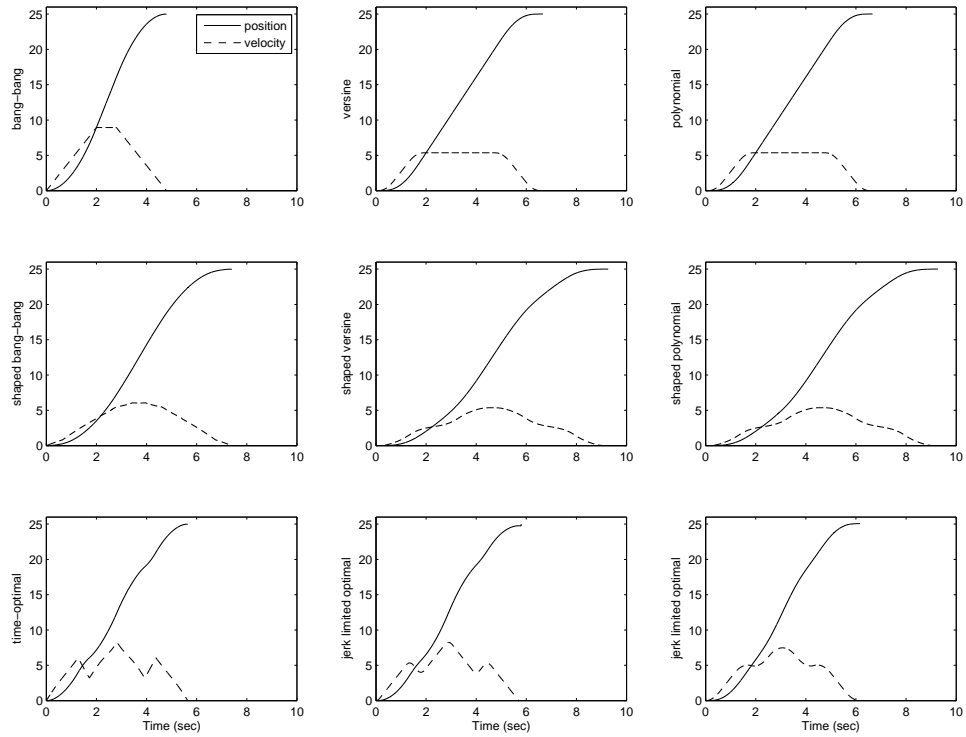


Figure 18. Reference Trajectory

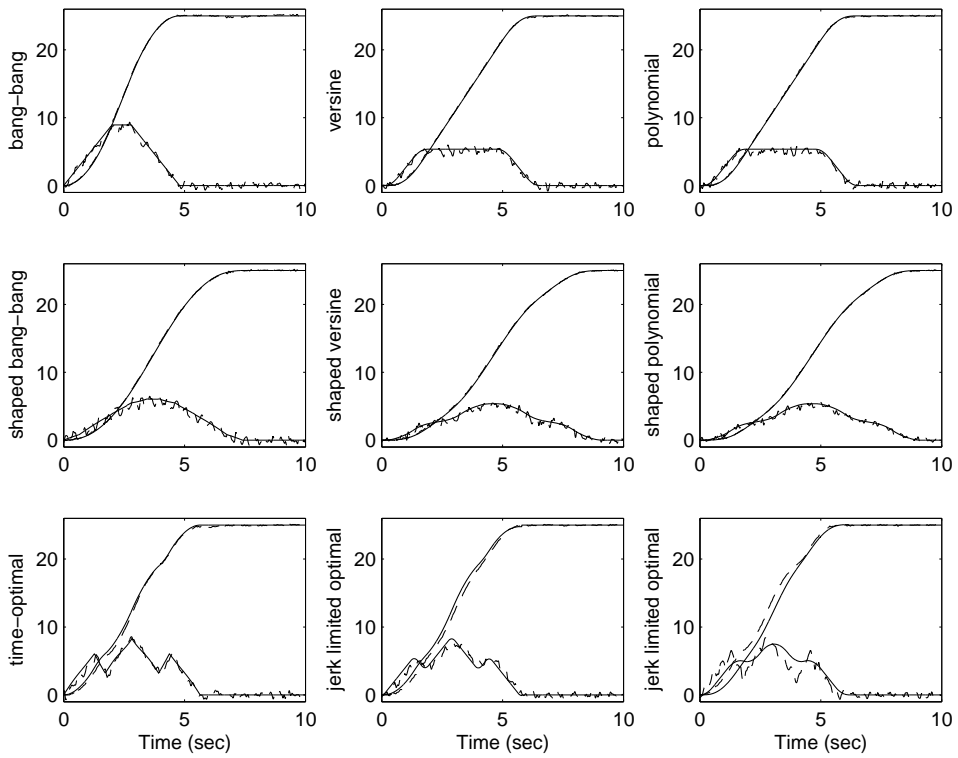


Figure 19. FSS Responses from Experiments

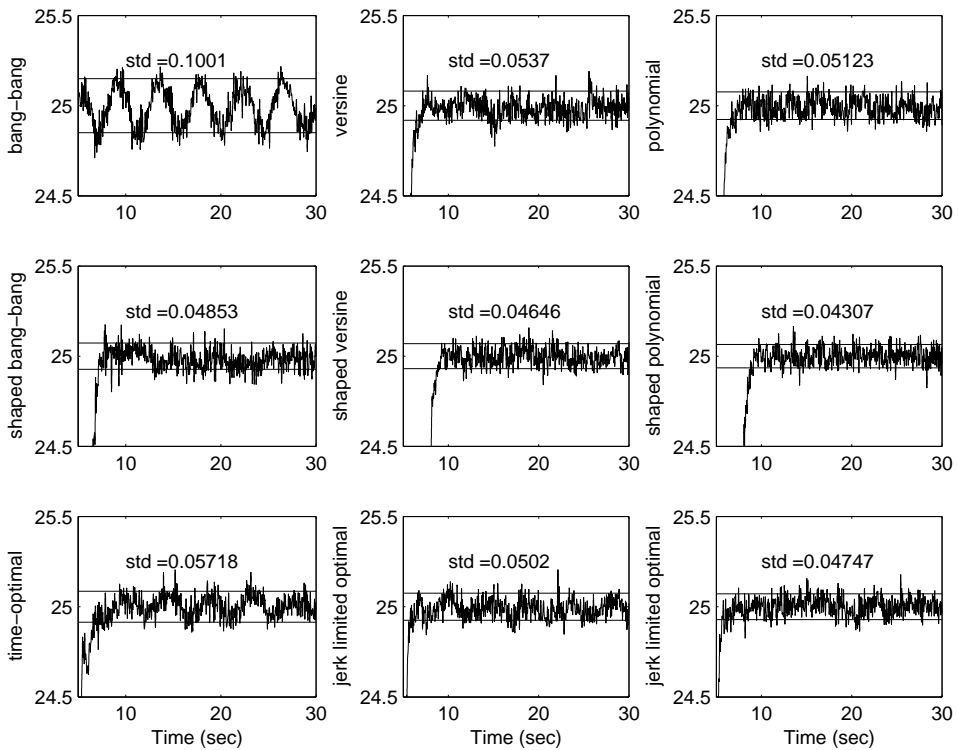


Figure 20. FSS Hub Angular Position Error

VI. Conclusion and Future Research

In the investigation, both the simulation and experimental results are presented to show the effectiveness of various jerk limited control profiles to reduce the vibration of the flexible spacecraft structure. The results suggest that the jerk limited rigid-body control profile such as versine or polynomial profile is effective to reduce the excitation of the flexible modes, however, better performance can be obtained from the handling of the low frequency modes as in input shaped and jerk limited optimal control profiles. The input shaping technique provided simple solution for exact cancellation of the known frequency modes. Although robustness to the frequency variation is not mentioned in this paper, desensitized input shapers are also well suited for the spacecraft slew maneuver application. The final time can be further decreased with the jerk limited optimal control profile with the added complexity of parameter optimization with reasonable prior knowledge of the control profile.

References

¹Junkins, J. L., Rahman, Z., and Bang, H., "Near Minimum-Time Maneuvers of Flexible Vehicles: A Liapunov Control Law Design Method", Mechanics and Control of Large Flexible Structures, Progress in Astronautics and Aeronautics, Vol. 129, 1990, pp. 565-593.

²Hailey, J. A., "Experimental Verification of Attitude Control Techniques for Flexible Spacecraft Slew Maneuver", Master Thesis, U.S. Naval Postgraduate School, March, 1992.

³Singer, N. C., and Seering, W. P., "Preshaping Command Inputs to Reduce System Vibration", Journal of Dynamic Systems, Measurement, and Control, Vol. 112, March 1990, pp. 76-82.

⁴Muenchhof, M., and Singh, T., 2003. Jerk Limited Time Optimal Control of Flexible Structures. "ASME Journal of Dynamic Systems Measurement and Control", Vol. 125, No. 1, 2003, pp. 139-142.

⁵Pao, L. Y., and Singhose, W. E., "On the Equivalence of Minimum Time Input Shaping with Traditional Time-Optimal Control " Proceedings of the 4th IEEE Conference on Control Applications, Albany, NY, September 1995, pp. 1120-1125

⁶Chen, H., and Agrawal, B. "Methods of Slewing the Spacecraft to Minimize Slewing Time", AIAA Guidance, Navigation, and Control Conference and Exhibition, Monterey, California, August 5-8, 2002.